Proceedings of the 2000 IEEE
International Conference on Control Applications
Anchorage, Alaska, USA • September 25-27, 2000

Design of an Acceleration Rate Controller for a Linear Drive of a Vertical Transportation System

M. Platen, D. Brakensiek, G. Henneberger
Institut für Elektrische Maschinen, RWTH Aachen, D-52056 Aachen, Germany
platen@iem.rwth-aachen.de

Abstract

In this paper a control system with an acceleration rate controller for a linear drive of a hoisting system is presented. The control system consists of a closed-loop speed control with inner acceleration rate control loop and current control loop. A simulation model established for analysis and optimization of the system is described and verified. The control parameters derived from the simulation are implemented on a model of the hoisting system equipped with the linear drive. The driving performance of the linear drive with acceleration rate controller is compared to a more simple controller structure with closed loop speed control and inner current control loop.

1 Introduction

An important criterion for a vertical transportation system is the smoothness of motion of the drive. The control system has to be designed according to this requirement. A simple closed-loop speed control with inner current control loop can be a suitable control system for a linear motor driving a hoisting system [1]. In the work presented in this paper an acceleration rate controller is added to that two-stage cascade controller as a middle cascade to achieve a further optimization of the dynamic performance of the system.

2 The Linear Motor

Various kinds of linear motors have been used as drives for vertical transportation systems [2], [3], [4]. The motor type chosen is a long-stator permanent-field linear synchronous motor. The layout has been optimized by finite element computation [5]. The motor has two peculiarities: The coils are ironless to minimize the normal forces of the motor. Furthermore, the permanent magnets are chamfered to reduce the ripple of the propulsion force. Fig. 1 shows the geometry of the motor. The stator coils are fixed to the hoistway by holding stems and cast resin. The permanent magnets and the iron yokes are mounted to the cage.

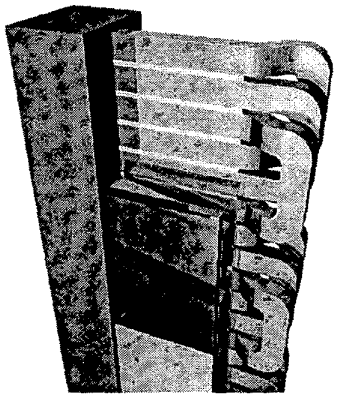

Figure 1: The geometry of the linear motor.

Static measurements of the propulsion force are taken from a model of the hoisting system equipped with the designed linear motor. The measured ripple of the propulsion force is smaller than 3 % of its mean value. In the working range of the motor the propulsion force is a linear function of the current fed to the stator coils.

3 Modelling

3.1 Mechanical System

A central point of modelling the hoisting system is a detailed description of the mechanical part of the system. Due to its construction it can be modelled by a spring-mass-system consisting of three masses connected by springs and dampers. The mechanical system is described by the dynamic equilibrium of forces for each mass, which is given by the following differential equation system:

$$F_p = m_m\ddot{s}_m + m_m g + C(s_m + s_c) + K(\dot{s}_m + \dot{s}_c) \quad (1)$$

$$C(s_m + s_c) + K(\dot{s}_m + \dot{s}_c) = m_c\ddot{s}_c + m_c g + F_f(v_c) \quad (2)$$

$$m_{cl}\ddot{s}_{cl} = -C_{cl}s_{cl} - K_{cl}\dot{s}_{cl} - F_p - m_{cl}g \quad (3)$$

Fig. 2 shows the block diagram of the mechanical model of the cage. The three masses of the system are the

0-7803-6562-3/00$10.00©2000 IEEE

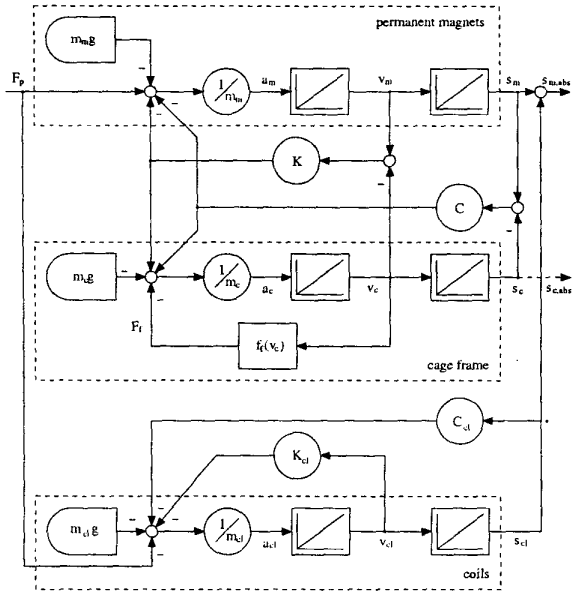

Figure 2: Block diagram of the mechanical model of the cage.

mass of the permanent magnets m_m, the mass of the cage frame m_c and the mass of the coils m_{cl}. The link of the masses m_m and m_c is modelled by a spring constant C and a damper constant K.

The propulsion force F_p acts according to *actio = reactio* on both, the mass of the permanent magnets m_m and the mass of the coils m_{cl}. The coils are not infinitely stiff so they can sag similar to a transverse beam. The rigidity of the coils is described by a spring constant C_{cl} and a damper constant K_{cl}. The sag of the coils is added to the relative movement of the permanent magnets s_m to obtain the absolute movement $s_{m,abs}$ of the permanent magnets, which is detected with a position encoder in the real system. In the model it is possible to detect the position of the permanent magnets as well as the position of the cage frame.

The spring bias of the coil spring and of the cage spring is taken into account by an initial deflection of the springs. This initial deflection can be derived from the static equilibrium of forces at the beginning of the simulation process.

3.2 Model of the Plant

Fig. 3 shows the block diagram of the plant. The linear motor is modelled by a constant factor k_m that calculates the force corresponding to the current. The variations of the propulsion force of less than 3 % are taken into account by a sinusoidal oscillation $f_r\,(s_m)$ with a period of electrical 60° that is added to the propulsion force of the motor. The position encoder is modelled as a quantizer $f_q\,(s_m)$ with the quantizing levels set according to the resolution of the encoder.

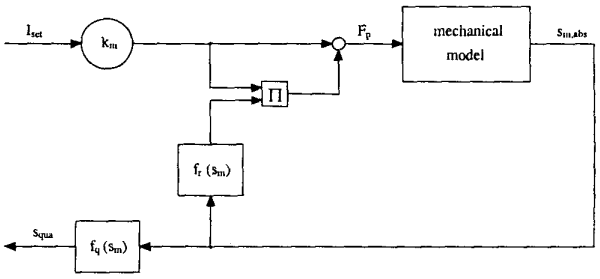

Figure 3: Block diagram of the plant.

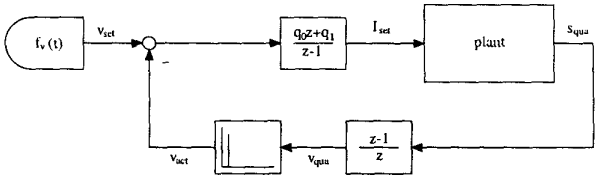

Figure 4: Controller structure of the speed controller.

4 The Speed Controller

4.1 Controller Structure

To verify the modelling of the mechanical system and the plant, a simulation of the hoisting system with a closed-loop speed control and inner current control loop is carried out.

Fig. 4 shows the structure of the speed controller. The influence of the inner current controller is not modelled, because its scanning frequency is much higher than the one of the speed controller. Therefore, the current controller has no influence on the driving performance of the hoisting system. The difference between the set-point value of the speed v_{set} and the actual speed v_{act} is given to the speed controller that calculates the set-point value of the current I_{set} required to move the cage. The position signal s_{qua} received from the plant is differentiated and filtered to obtain the actual speed.

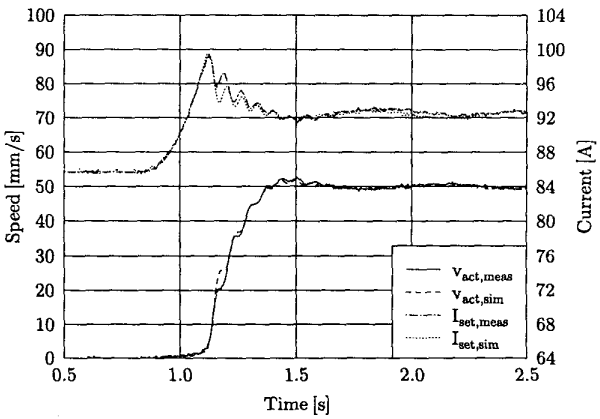

Figure 5: Comparison of simulation to measurement.

4.2 Simulation

The parameters of the mechanical system are set in a way, that measurements and simulation results correspond to each other. Fig. 5 shows the current and the speed for a starting up from 0 mm/s to 50 mm/s. The position is measured on the permanent magnets. Measurements and simulation results show a good correspondence.

The current and the speed show three effects: The quantizing noise caused by the resolution of the position encoder is visible. Furthermore, the small variations of the speed caused by the ripple of the propulsion force can be detected. The fading oscillation at the starting is caused by vibrations of the three-mass-system of the cage.

Simulation results and measurements correspond for the same set of parameters when measuring the position on the cage frame.

5 The Acceleration Rate Controller

5.1 Controller Structure

To improve the driving performance of the cage an acceleration rate controller is introduced. Fig. 6 shows the controller structure.

The acceleration rate controller is added to the cascade control with speed controller and current controller as middle cascade. The current controller is neglected again in the modelling. The analog acceleration signal a_{ana} is derived from a capacitive accelerometer that is positioned on top of the permanent magnets. An analog 4th-order Butterworth filter with a cut-off frequency of 200 Hz suppresses the noise. After digitizing the acceleration signal is filtered again to restrain the quantizing noise.

The speed controller and the acceleration rate controller are implemented as digital PI controllers. The transfer function of a digital PI controller is:

$$G_{PI}(z) = \frac{q_0 z + q_1}{z-1} = q_0 + (q_0 + q_1)\frac{1}{z-1} \qquad (4)$$

The term q_0 is the proportional part of the controller

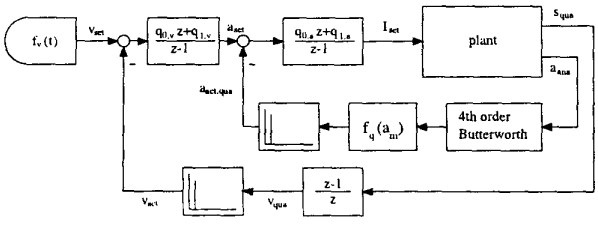

Figure 6: Controller structure with speed control and inner acceleration rate controller.

Table 1: Chosen set of controller parameters.

K_{Rv}	25
T_{Iv}	20
K_{Ra}	0,002
T_{Ia}	0,003

and the term $q_0 + q_1$ is the integral part. An analog PI controller, whose parameters K_R and T_I describe the controller entirely, has the transfer function:

$$G_{PI}(s) = K_R + \frac{1}{s} \cdot \frac{K_R}{T_I}, \qquad (5)$$

with $q_0 = K_R$ and $q_1 = K_R(\frac{T}{T_I} - 1)$ and $\frac{1}{T}$ being the scanning frequency. Only the parameters of the analog controller, K_R and T_I, are accessible from outside.

5.2 Controller Parameterization

The parameterization of K_{Rv}, T_{Iv}, K_{Ra} and T_{Ia} is optimized by means of simulation. In a first step the speed control loop is opened, and the acceleration rate controller is optimized. An arbitrary function a_{set}, for example a jump function, is used, and the parameters of the controller are adjusted in a way, that a_{set} and $a_{act,qua}$ correspond to each other. The same procedure is done for the outer control loop with the chosen inner loop parameters. The chosen set of parameters is displayed in Table 1.

6 Measurements

6.1 The Experimental Arrangement

The set of parameters derived from the simulation is implemented on a model of the hoisting system. Fig. 7 shows the structure of the test bench. The speed control is implemented on a Texas Instruments TMS 320 C 30 DSP with a clock-pulse rate of 16 MHz. The PC communicates with the DSP via a dual ported RAM. The analog outputs of the DSP card are used to transmit the setpoint values of the current I_d and I_q to the current controller. The currents I_d and I_q are generated from the setpoint value of the current amplitude by modulating it with the electrical angle. The linear motor is fed by a three phase voltage source converter.

The position of the cage is detected by an incremental rotary position encoder. The incremental position signals of the position encoder are evaluated by a position recording card, that counts the sent impulses. The acceleration of the cage is detected by an accelerometer fastened on top of the permanent magnets. The acceleration signal is conditioned by an acceleration processing card.

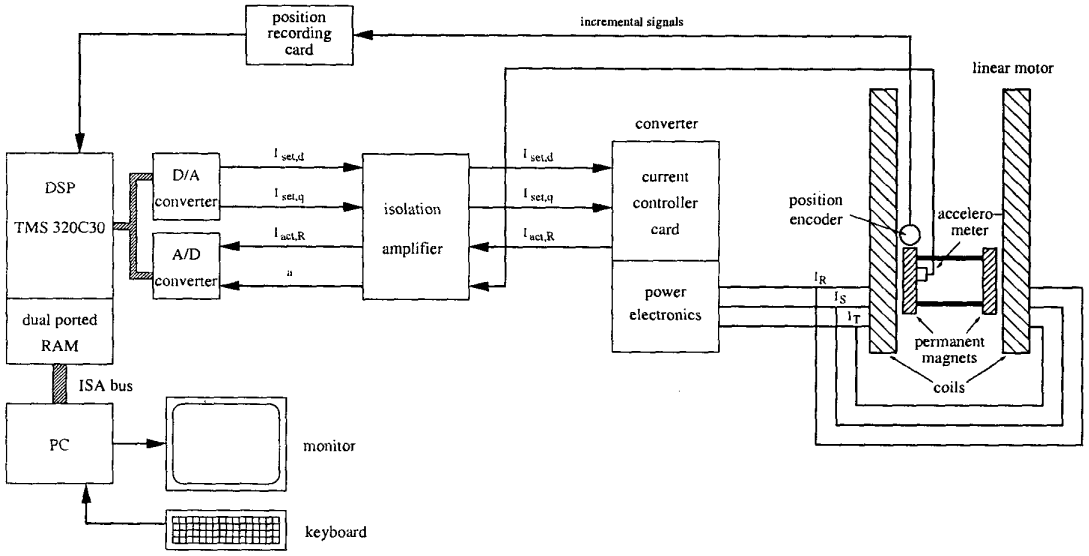

Figure 7: Structure of the test bench.

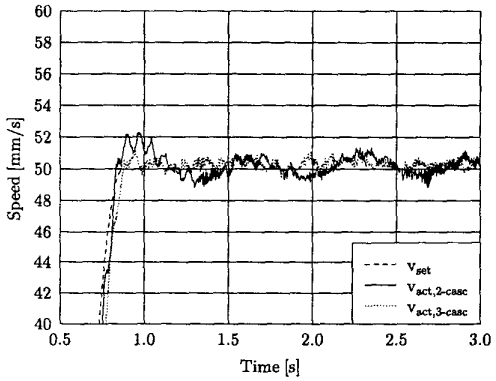

Figure 8: Measured speed signal for the two-stage cascade controller and for the three-stage cascade controller.

6.2 Results

Fig. 8 shows the measured speed signal of the hoisting system with the two-stage cascade controller and with the three-stage cascade controller for a starting up from 0 mm/s to 50 mm/s. The use of an acceleration rate controller allows for a faster correction of deviations. This is because the analog acceleration rate signal is available faster than the speed signal. The fading oscillation at the starting due to the vibrations of the three-mass-system as well as the variations of the speed caused by the ripple of the propulsion force are reduced significantly.

7 Conclusions

The described simulation model consisting of a spring-mass-system with three masses allows for a quite detailed simulation of the low-frequency performance of the examined hoisting system. In comparison to a closed-loop speed control with inner current control loop, the driving performance of the linear drive is improved by implementing an acceleration rate controller. The overshoot as well as the deviation of the speed signal are reduced significantly.

References

[1] M. Platen and G. Henneberger, "Controller design for a linear drive of a hoisting system", *IECON'99 - The 25th Annual Conference of the IEEE Industrial Electronics Society*, vol. 3, pp. 1477-1480, 1999.

[2] J. F. Gieras, E. Gagnon, Z. Piech, Z. Jian, "Innovative elevator drive with a linear induction motor" *International Conference on Power Electronics and Electrical Drives (ED&PE'92)*, pp. 150-155, 1992.

[3] T. Morizane, E. Masada, H. Ohsaki, M. Tamura, "Vertical motion direct drive with linear induction motor" *International Power Electronics Conference (IPEC'95)*, vol. 1, no. 3,1, pp. 557-562, 1995.

[4] M. Miyatake, N. Ishikawa, T. Koseki and S. Sone, "Experimental and operational study on vertical transportation system driven by a linear synchronous motor using permanent magnets", *Linear Drives for Industry Applications (LDIA'95)*, pp. 73-76, 1995.

[5] M. Platen, W. Evers and G. Henneberger, "A linear synchronous motor for a vertical transportation system - numerical calculations and test results", *8th International IGTE Symposium on Numerical Field Calculation in Electrical Engineering*, pp. 571-574, 1998.